



Research article

Highly sensitive and quantitative HiBiT-tagged Nipah virus-like particles: A platform for rapid antibody neutralization studies

Arathi Rajan^a, Anuja S. Nair^a, Vinod Soman Pillai^a, Binod Kumar^b,
Anupama R. Pai^a, Bimitha Benny^a, Mohanan Valiya Veetil^{a,*}

^a Department of General Virology, Institute of Advanced Virology (IAV), Kerala, 695317, India

^b Department of Antiviral Research, Institute of Advanced Virology (IAV), Kerala, 695317, India

ARTICLE INFO

Keywords:

Nipah virus
Nipah virus-like particles
NanoBiT technology
Rapid luminescence assay

ABSTRACT

Biocontainment regulations restrict the research on NiV to BSL-4 laboratories, thus limiting the mechanistic studies related to viral entry and allied pathogenesis. Understanding the precise process of viral-particle production and host cell entry is critical for designing targeted therapies or particle-based vaccines. In this study, we have synthesized HiBiT-tagged-NiV-VLPs to ease *in-vitro* BSL-2 particle handling. We propose a simple yet effective approach of generating substantial amount of HiBiT-tagged NiV-VLPs *in vitro* by co-expressing viral structural proteins in HEK293T cells. Though homologous to parent virus, the incapacitated replication potential facilitates a BSL-2 handling of these particles. The inclusion of a highly sensitive HiBiT tag on these VLPs allows for a quick detection of viral binding and entry, as well as in assessing the efficiency of neutralizing antibodies *in vitro* using the NanoBiT technology. The HiBiT-tag binds in high affinity with LgBiT (Large BiT an 18 kDa fusion protein and complementary subunit of HiBiT peptide), and the resultant complex elicits high intensity luminescence in the presence of substrate. The VLPs produced were morphologically and functionally identical to the native virus, and the HiBiT-tag permitted their quick application in viral binding, entry, and antibody neutralization assays.

“Thus, we report a simple setting for generating HiBiT-NiV VLPs which can be utilized in a BSL-2 laboratory, to concurrently quantify features of NiV assembly, binding and entry. This also offers an alternate-safe and effective platform for viral based antibody neutralization assays *in vitro*”.

1. Introduction

The zoonotic virus Nipah (NiV), first identified in Malaysia during 1990s, is a highly pathogenic and incredibly fatal *paramyxovirus*, accounted to cause respiratory ailments, neurological disorders and severe vascular damage, with case fatality rates up to 80 % in affected humans and animals [1,2]. NiV has a wider host range accounting for massive outbreaks, devastating livestock loss and socio-economic consequences over the past 24 years since its discovery. Though a few antiviral drugs have shown potential activity in small animal models and human primates, no specific therapeutics or antivirals have been approved for treatment of human infections [3,4]. Understanding the biology of viral infection and developing novel tools to assess the efficiency of antibodies or antivirals would

* Corresponding author.

E-mail address: mohanveetil@iav.res.in (M.V. Veetil).

<https://doi.org/10.1016/j.heliyon.2024.e31905>

Received 17 November 2023; Received in revised form 6 May 2024; Accepted 23 May 2024

Available online 24 May 2024

2405-8440/© 2024 Published by Elsevier Ltd.

This is an open access article under the CC BY-NC-ND license

(<http://creativecommons.org/licenses/by-nc-nd/4.0/>).

provide vital insights into the treatment of NiV infection. However, the extreme level of biosafety precaution required for handling this BSL-4 pathogen confines the research on NiV. A more secure and cost-effective method of managing potent antigenic viral proteins in the laboratory would alleviate this dilemma.

Virus-Like Particles (VLPs) are such platforms gaining popularity in the field of vaccine virology and restorative medicine. VLPs are replication incompetent, polymerase deficient self-assembly of viral structural proteins, mimicking the native virus in its morphology, nature and antigenicity. In an equivalent manner, the co-expression and self-assembly of Nipah viral structural proteins ought to logically result in the release of nascent NiV-VLPs *in vitro* [5].

The genome of the NiV encodes six major proteins: glycoprotein (G), fusion protein (F), matrix (M), nucleocapsid (N), long polymerase (L) and phosphoprotein (P). The N, P, and L proteins are critical for the reconstitution of viral RNA polymerase activity, the matrix protein M is required for viral particle formation and budding, while, two surface glycoproteins G and F are vital for attachment and entry into the susceptible host cell [5–7].

In the current study, we have generated HiBiT tagged Nipah virus-like particles (NiV-VLPs) using plasmid-based expression systems encoding the NiV structural proteins G, F, and M, which allows their self-assembly into nascent NiV-VLPs when co-synthesized *in vitro*. The VLP-system is designed to express a fragment of the N-Luc, which is an 11 amino acid peptide tag called HiBiT, appended to the gene encoding M protein. This small HiBiT tag generates quantitative luminescence by high affinity complementation with the 18 kDa N-Luc component LgBiT [8–10]. The N-Luc based system allows an antibody-free system for assessing VLP assembly, release, titration, host cell binding and entry. The HiBiT tag also functions as a marker for evaluating live cell VLP entry kinetics, allowing it to be used in rapid antibody neutralization assays. Thus, the antigenicity and allied vaccine potential of these particles would serve as the base for future investigations involving *in vivo* models for not just NiV but also other potentially pathogenic viruses.

The sequential procedures involved in the purification and concentration of NiV-VLPs used in this work are modified and less arduous than the standard approach. Thus, the study's novelty resides in the creation of a less complicated and cost-effective method of generating substantial quantities of NiV-VLPs that might be employed in multitudinous viral-based *in vitro* (BSL-2) tests predominantly viral entry and antibody neutralization assays. While the notion of producing VLPs or tagged VLPs (e.g., HiBiT) can be applied to several enveloped viruses, BSL-3/4 viruses which are understudied due to their high pathogenicity, would gain the most from this approach due to the ease of handling these particles in BSL-2 laboratories.

2. Materials and methods

2.1. Cell lines and culture conditions

Human Embryonic Kidney cell line HEK293T(NCCS, Pune) and Human B lymphoma cell line RAJI (NCCS, Pune) were cultured respectively in DMEM (Gibco) and RPMI 1640 (Gibco) with 10 % Fetal Bovine Serum (FBS-Gibco) and 1 % Penicillin-Streptomycin (Sigma Aldrich) at 37°C in a CO₂ incubator. Human endothelial cell line TIVE-LTC (A kind gift from Dr. Rolf Renne, University of Florida) was cultured in EBM2 media with growth factors (Lonza) supplemented with 10 % Fetal Bovine Serum (FBS-Gibco). All the experiments employed exponentially growing cells with lower passages, and cell lines were subjected to periodic Mycoplasma testing.

2.2. Generation of plasmid -expression system and transfections

The codon optimized NiV B (Bangladesh strain: Genbank AY988601.1) structural proteins encoding G, F, and M gene blocks were synthesized by Biomatik (Singapore) and cloned into pcDNA3.1+ mammalian expression vector using the Kpn I and Not I restriction sites under the control of a CMV promoter. The gene encoding M protein was modified by appending a small 11 amino acid long peptide tag 'HiBiT' (VSGWRLFKKIS) using linker sequences (GSSGGSSG) either upstream or downstream of the gene (**Detailed in supplementary information S1A**). LgBiT expression vector (#N268A, Promega Corp.) was used for all N-Luc-based experiments. All transfections were performed using Lipofectamine™ 3000 Transfection Reagent (#L3000001, Invitrogen) as per the manufacturer's protocol. For generation of cell lines stably expressing LgBiT, clones were selected using specific concentration of antibiotic (#TC027 Hygromycin-HIMEDIA) for 45 days.

2.3. Generation and purification of NiV-VLPs

Exponentially growing HEK293T cells at a confluency of 80 % were transfected with equimolar concentrations of plasmids encoding NiV structural proteins F, G and HiBiT tagged M (In combinations of G-F or G-F-M), using lipofectamine 3000 as per the standard protocol. NiV-VLP containing cell supernatant (SUP) were harvested 48 h post transfection and exposed to sequential steps of clarification, purification and refining. Briefly, the harvested cell SUP was cleared by centrifugation at 3500 rpm at 4⁰ C for 30 min. The precleared SUP was concentrated by ultracentrifugation through a 20 % sucrose cushion in TN buffer (0.1 M NaCl; 0.05 M Tris-HCL, pH 7.4) at 30,000 rpm for 4 h, in a Beckman coulter centrifuge (#Optima XPN 100). The resultant pellet was resuspended in 0.5 ml of sterile, endotoxin free TN buffer and exposed to a subsequent cycle of ultracentrifugation through a 20 % sucrose cushion at 30000 rpm for 2 h. The concentrated VLP pellet was resuspended in 250 µl of sterile endotoxin free TN buffer and stored in aliquots of 50 µl for further experiments. The cell SUP harvested from HEK293T cells transfected with empty vector pcDNA3.1+ and processed in similar way are referred to as mock VLPs and were used as negative control as and when required. Owing to the pleomorphic nature of NiV and NiV-VLPs (NiV is a pleomorphic virus with irregularity in particle size ranging from 40 to 1900 nm [11,12]), the conventional practice of concentrating precleared SUP using MWCO filters, size exclusion chromatography and subsequent density gradient centrifugation

[5,13–16] had been eliminated and modified in the present study to minimize VLP-loss. On the basis of their N-Luc activity following LgBiT complementation, VLP inputs from different batches were normalized to Relative Light Units (RLU) for use in downstream experiments.

2.4. Western blot analysis and Co-Immunoprecipitation assays (CO-IP)

Whole cell lysates (WCL) were prepared by lysing the cells in RIPA lysis buffer with 1X protease/phosphatase inhibitor cocktail (CST #5872) at 4 °C. Purified VLPs or cell lysates were quantified using Bradford assay and denatured in 6X Laemmli sample buffer (375 mM Tris-HCl, 9 % SDS (w/v), 50 % glycerol (v/v), 0.03 % bromophenol blue (w/v) and 9 % beta-mercaptoethanol (v/v)) for 5 min at 95 °C, the samples were then separated on discontinuous SDS gel and transferred to nitrocellulose membranes (BioRad). The membranes were blocked using 5 % skimmed milk and probed with respective primary/HRP conjugated secondary antibodies and imaged by chemiluminescence based technique using BioRad Chem Doc XR⁺ System Vs Image Lab software.

For Co-IP experiments, 500-1000ug of VLP immunoprecipitated for 1 h at 4 °C with IP specific NiV G/F antibodies were then incubated with Rec-protein A/G sepharose beads (Invitrogen) overnight at 4 °C with shaking. The samples were denatured in 6X Laemmli sample buffer for 5 min. The supernatant was spun at 3500 rpm and resolved using a 10 % SDS-polyacrylamide gel and immunoblotted using IP specific antibodies. Normal mouse IgG (Santa Cruz) was used as control for pull down, and 10 % non-immunoprecipitated proteins served as inputs.

All the HiBiT-tagged proteins were detected using the Nano-Glo HiBiT blotting system (Promega) with exogenous supply of 20 µg of LgBiT protein in the blotting buffer, referred to as 'HiBiT blotting'.

2.5. Immunocytochemistry/immunofluorescence analysis

Immunocytochemical analysis was performed as described elsewhere [17]. Briefly, the cells after respective treatments or VLP infection were fixed at -20 °C in Acetone: Methanol, blocked with 3 % Bovine Serum Albumin (Sigma Aldrich, USA) and probed with primary antibodies overnight at 4 °C. Unbound antibody fractions were removed with 1X PBS, probed with Alexa Flour-conjugated secondary antibodies at room temperature, counterstained and mounted using DAPI containing mountant (Sigma Aldrich). Observed under ZEISS Axio Vert.A1 fluorescence microscope and images were processed using ZEISS-ZEN microscopy software.

2.6. Electron microscopic analysis

Purified NiV-VLPs were adsorbed on to formvar carbon coated copper grids (FF400-Cu) by drop floatation for 30 min, blot dried and imaged using JEOL-JEM 1010 transmission electron microscope (TEM) (100K magnification).

2.7. Nano Luc based split luciferase assays for NiV-VLP binding and entry (N-LucAssay)

For this study, a split luciferase assay designed around NanoLuc (N-Luc) was utilized. N-Luc is a luminescent protein with low molecular weight and high luminescence activity. Based on the Nono Binary Technology the N-Luc can be separated into two subunits; 18 kDa LgBiT and 1.3 kDa HiBiT with higher complementarity to each other [10,18]. Because of the low dissociation constant (Kd) and greater binding affinity of these subunits, the system is utilized in Luciferase-based experiments.

For all cell binding assays, exponentially growing cells (stably expressing or not expressing LgBiT subunit) at a confluency of 80 % were infected with 5000 RLU of HiBiT-tagged NiV VLPs or mock particles for 1 h at 4 °C. Following infection, cells were either washed and fixed for immunofluorescence examination of NiV-glycoproteins (G/F) or lysed in Nano-Glo luciferase assay buffer and the resulting N-Luc activity was measured using the Nano-Glo luciferase assay system (Promega #N1110). The luminescence intensities were determined using the Promega GloMax(R) Multi-detection System, and the normalized luminescence intensities were expressed in Relative Light Units (RLU).

For all in situ live cell assays, exponentially growing cells with stable expression of LgBiT were treated with definite units of N-Luc live cell substrate vivazine (Promega, #N2580) and incubated at 37 °C, as per manufacturer's protocol. The cells were subsequently infected with HiBiT-tagged NiV-VLP-2/mock in doses of 5000 RLU and incubated at 37 °C for 4 h so as to enable VLP entry. The N-Luc activity, an immediate indicator of VLP entry kinetics, was measured every 30 min with a Promega GloMax (R) Multi-detection System.

Parallely a set of cells exposed to same experimental conditions were lysed at 2 h using Nano-Glo lysis buffer to facilitate a maximum HiBiT:LgBiT complementation. The proportions of NiV-VLPs that entered the cells at different time points after detergent cell lysis were then compared to the data from live cell assay, and normalized luminescence intensities were expressed as Relative Light Units (RLU). Mock infected cells as well as cells not expressing LgBiT served as respective controls for these assays. Exogenous supply of 20 µg LgBiT protein was used for all lytic N-Luc assays-performed with cells not expressing LgBiT.

2.8. Antibody neutralization assays

5000 RLU of HiBiT-Tagged NiV-VLP-2/mock was preincubated at 37 °C with 2, 5, and 10 µg of neutralizing (Ab02863-1.1, Absolute Antibody) or non-neutralizing monoclonal antibodies (MAB1236-100, Native antigen) specific to NiV G. Following neutralization, the VLP entry was investigated at different time intervals in HEK293T and TIVE-LTC cells using the live cell/lytic N-Luc assays as previously documented.

2.9. Statistical analysis

All experiments were performed in triplicates and the values are expressed as mean \pm SD from at least three independent experiments. The error bars are calculated on the basis of the SD values. ANOVA or unpaired two-tailed student's t-test were employed to determine the likelihood of significant differences between different experimental groups. Statistical analyses were performed using GraphPad Prism 8 (USA). * $P \leq 0.05$ was perceived statistically significant; ns-non significant.

Table 1 details all of the reagents, kits, antibodies, cell lines, software and algorithms that have been used in the present study.

Table 1
Key Resources Table

| REAGENT or RESOURCE | SOURCE | IDENTIFIER |
|----------------------------------------------------------------------------------------|---------------------------------------------|-----------------------------------------------------------------|
| Antibodies | | |
| Anti-Hendra and Nipah virus G | Absolute Antibody | Ab02863-1.1 |
| Anti-Nipah virus F F1 | Absolute antibody | 5G7 |
| Mouse Anti-Nipah Virus Glycoprotein G Antibody (AE6) for ICC | Native Antigen | MAB1236-100 |
| Mouse Anti-Nipah Virus Glycoprotein F Antibody (CG11) for ICC | Native Antigen | MAB12307-100 |
| Anti-LgBiT Monoclonal Antibody | Promega Corp. | N710A |
| β -Actin Rabbit mAb (High Dilution) | Abclonal | AC026 |
| Goat anti-Mouse IgG (H + L) Cross-Adsorbed Secondary Antibody, Alexa Fluor™ 488 | Invitrogen | A32723 |
| Goat anti-Mouse IgG (H + L) Highly Cross-Adsorbed Secondary Antibody, Alexa Fluor™ 594 | Invitrogen | A11005 |
| Goat anti-Mouse IgG (H + L), Secondary antibody HRP | Invitrogen | 31430 |
| Normal Mouse IgG | Santa Cruz Biotechnology | Sc-3877 |
| Biological samples | | |
| NIL | | |
| Chemicals, peptides, and recombinant proteins | | |
| RIPA Lysis Buffer | HIMEDIA | TCL131 |
| Protease/Phosphatase Inhibitor Cocktail (100X) | Cell Signaling Technology | 5872 |
| Lipofectamine 3000 transfection reagent | Invitrogen | L3000001 |
| Hygromycin B | HIMEDIA | TC027 |
| Bio-Rad Protein Assay Dye Reagent Concentrate | Bio Rad | 5000006 |
| Sucrose | Sigma Aldrich | S0389 |
| TRISMA Base | Sigma Aldrich | 77-86-1 |
| Pierce™ IP Lysis Buffer | Thermo Scientific | 87787 |
| Mounting Medium with DAPI | Sigma Aldrich | DUO82040 |
| Rec-protein A sepharose beads | Thermo Scientific | 101141 |
| Rec-protein G sepharose beads | Thermo Scientific | 101241 |
| FastDigest <i>Kpn</i> I | Thermo Scientific | FD0524 |
| FastDigest <i>Not</i> I | Thermo Scientific | FD0593 |
| Critical commercial assays | | |
| Nano-Glo® Live Cell Assay System | Promega Corp. | N2580 |
| Nano-Glo luciferase assay system | Promega Corp. | N1110 |
| Deposited data | | |
| NIL | | |
| Experimental models: Cell lines | | |
| HEK293T | NCCS, Pune | |
| TIVE-LTC | Dr. Rolf Renne, University of South Florida | |
| RAJI | NCCS, Pune | |
| Experimental models: Organisms/strains | | |
| NIL | | |
| Oligonucleotides | | |
| NIL | | |
| Recombinant DNA | | |
| Details of plasmid DNAs used in the study are detailed in Supplementary information 1 | | |
| Software and algorithms | | |
| Image Lab software | Biorad | https://www.Bio-Rad.com |
| Adobe Photoshop 2022 | Adobe | https://www.adobe.com |
| Graph Pad Prism 8 | Dotmatics | https://www.graphpad.com |
| Zeiss Zen Microscopy software | Zeiss | https://www.zeiss.com |
| EndNote X9 | Clarivate Analytics | https://endnote.com |
| Other | | |
| NIL | | |

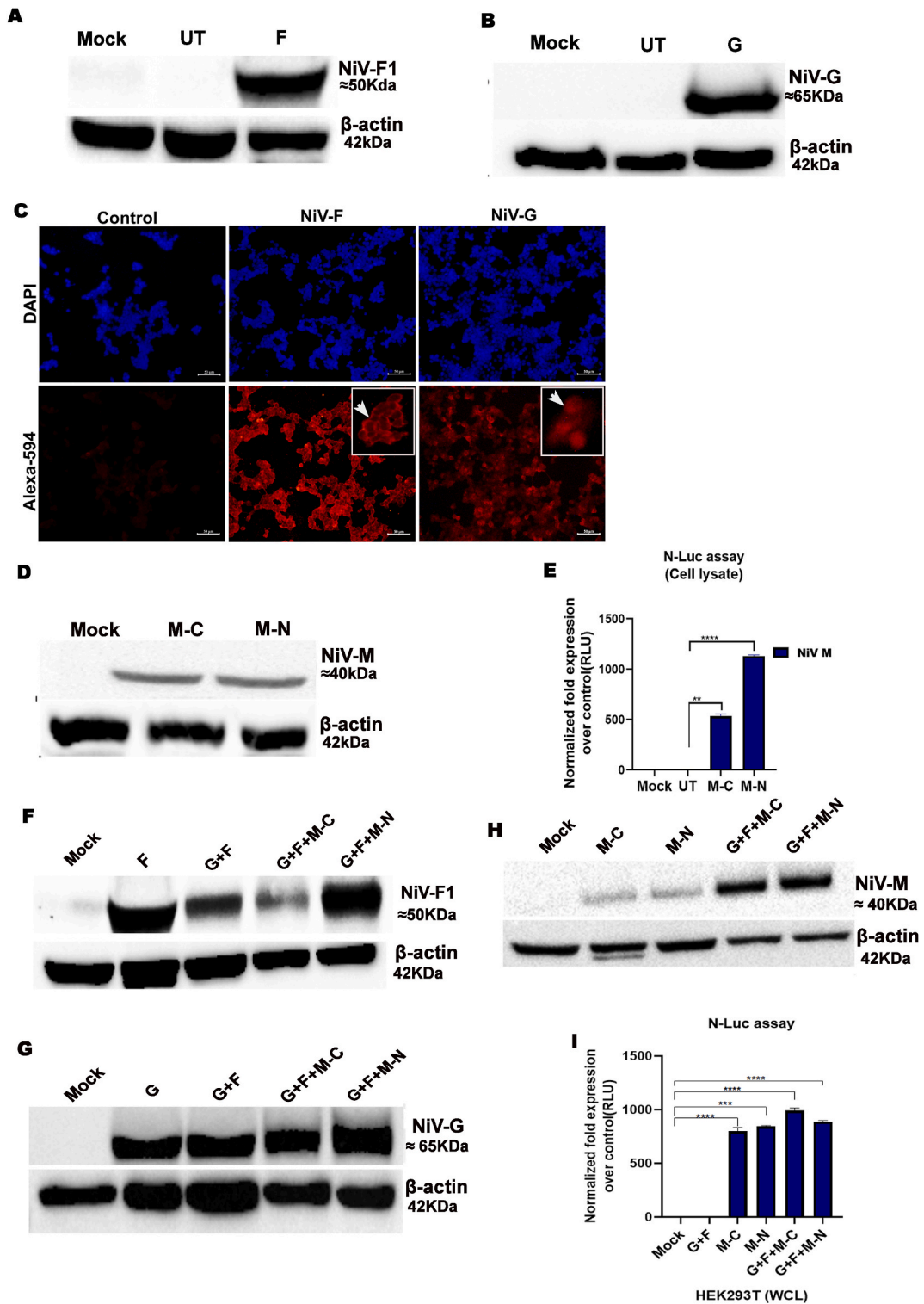


Fig. 1. NiV structural proteins co-express and self-assemble to generate VLPs *in vitro*. HEK293T cells were transfected with NiV-F, G and M encoding plasmids and the protein expression levels were analyzed in cell lysates 48 h post transfection. Expression of NiV F and G protein detected by Western blot analysis using NiV-F1 (≈50 kDa) and NiV G (≈65 kDa) specific antibodies (A, B). Un-transfected cells (UT) and cells transfected with empty vector pcDNA3.1 served as the control/mock. β-actin served as the endogenous control for Western blot, (C) Immunofluorescence analysis showing the expression of NiV F and NiV G proteins. Arrow marks in boxed area indicate NiV F and NiV G expression. (20X/scale bar 50 μm). (D) HiBiT blot for NiV-M protein; NiV-M-C and NiV-M-N respectively represent the M

expression vectors with HiBiT tag on C-terminal and N-Terminal ends. 48 h post transfection cell lysates were subjected to HiBiT blotting using reagents containing 20 µg LgBiT protein and N-Luc substrate. **(E)** HEK293T cells were transfected with HiBiT tagged NiV-M-C and NiV-M-N plasmids, and the expression of the HiBiT tagged protein were analyzed 48 h post transfection in cell lysate by N-Luc based split luciferase assay. The luminescence intensities were normalized to respective controls and are expressed as RLU (Relative Luminescence Unit). HEK293T cells were transfected individually with either NiV-F, G, M-C/M-N expression plasmids or in combinations of G + F, G + F + M - C or G + F + M-N. 48 h post transfection, expression of NiV F **(F)** and NiV-G **(G)** proteins were analyzed by Western blot analysis using antibody specific to NiV F1 and NiV G. Expression levels of HiBiT tagged NiV-M-C and NiV-M-N proteins in the cell lysates were analyzed by HiBiT blotting **(H)** and N-Luc assay **(I)** using 20 µg LgBiT protein and its substrate. **(J) Schematic representation of the *in vitro* self-assembly of NiV proteins and release of HiBiT tagged NiV-VLPs.** Cells co-transfected with G, F, and M-C/M-N expression plasmids would promote their co-expression inside the cells, resulting in their self-assembly to generate NiV-Virus Like Particles (NiV-VLPs). Combinations of G + F, G + F + M-C or G + F + M-N are used for the transfection, thus the G + F VLPs and HiBiT tagged G + F + M-C/M-N VLPs generated; and are respectively referred as NiV-VLP-1 and NiV-VLP-2. The VLPs will be released in substantial amounts extracellularly to the culture supernatant 48 h post transfection. The Supernatant harvested is purified using a simplified 3-step process for downstream experiments. Lower panel explains how the HiBiT tag on the VLP functions: **(1)** HiBiT, an 11 amino acid peptide tag attached to the gene encoding M protein facilitates the production of HiBiT Tagged VLPs. **(2)** Which upon infecting a cell expressing LgBiT, would facilitate the HiBiT:LgBiT complementation and production of **(3)** NanoBiT peptide releasing Nano Luciferase, the resultant luminescence signal enables us with an antibody-free detection system in presence of a substrate. **(K)** Culture supernatants from HEK293T cells transfected with G + F or G + F + M were procured 48h post transfection, clarified by centrifugation and concentrated using Amicon MWCO filters. HEK293T cells stably expressing LgBiT protein were infected with the clarified concentrate, the luminescence intensity was measured using the NanoLuc assay. **(L)** The supernatant from NiV G + F, M, G + F + M co-transfected cells were collected 48h post transfection, and analyzed for the expression of NiV-M proteins by NanoLuc assay. (Error bars, mean ± SD, *P ≤ 0.05, **P ≤ 0.005,***P ≤ 0.001, and ****P ≤ 0.0001, unpaired t-test). (Uncropped/non-adjusted versions of western images are provided in supplementary information S3. Red boxes denote cropped images that are presented in the manuscript. (For interpretation of the references to colour in this figure legend, the reader is referred to the Web version of this article.)

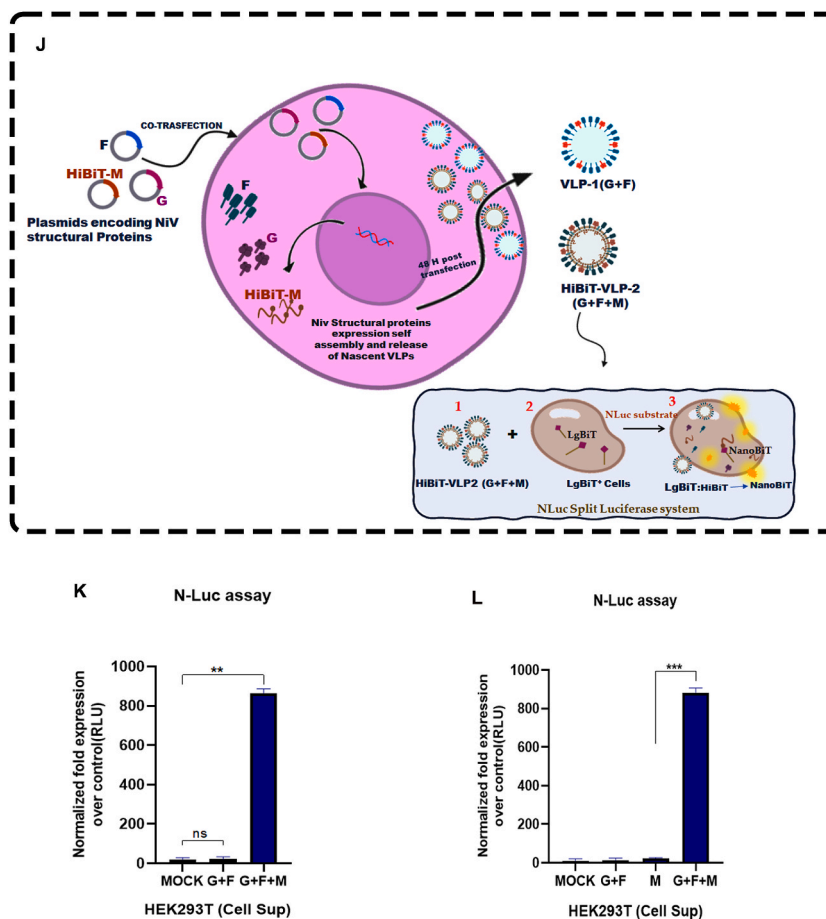


Fig. 1. (continued).

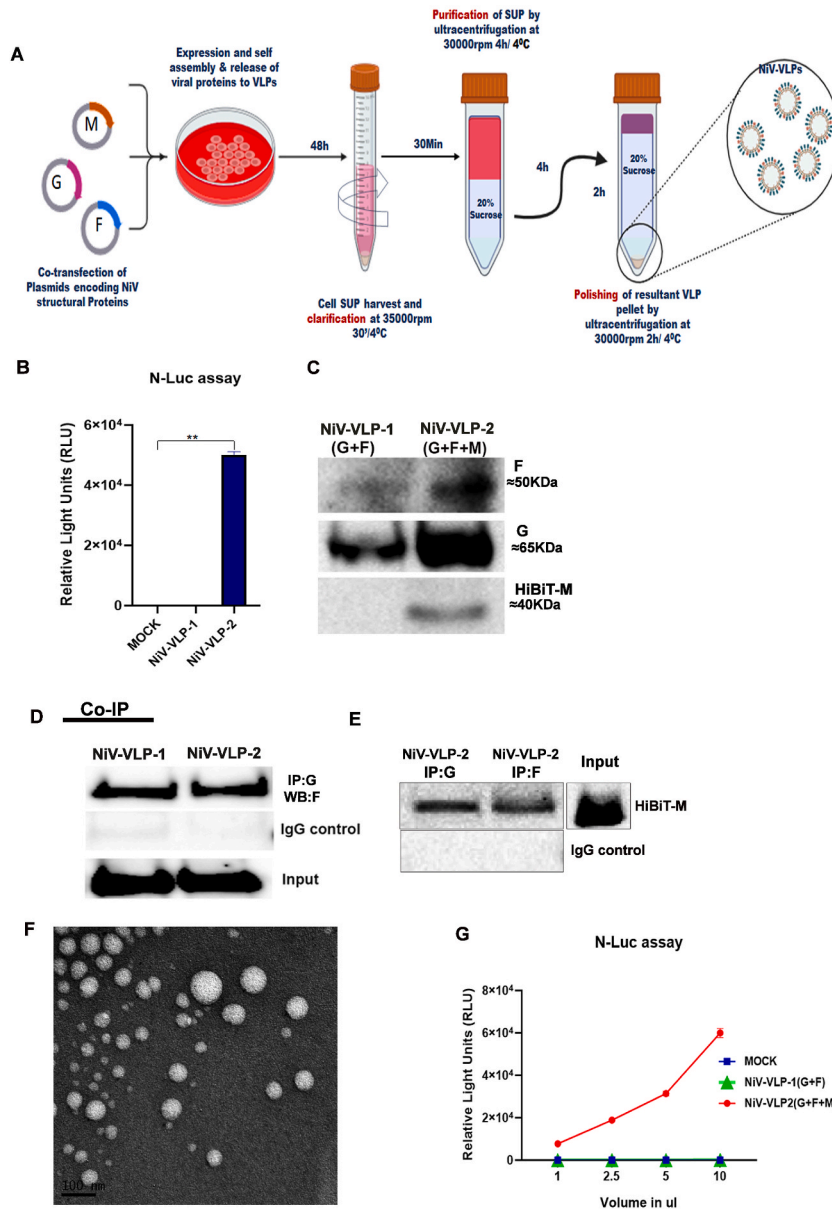


Fig. 2. Synthesis, purification and characterization of NiV-VLPs

(A). Schematic representation of harvesting and purifying NiV-VLPs (NiV-VLP1/G + M and NiV-VLP2/G + F + M). The VLPs were extracted and clarified from transfected-cell supernatant by centrifugation at 3500 rpm for 30 min at 4 °C. The cleared supernatants were concentrated and purified by ultracentrifugation at 30000 RPM for 4 h at 4 °C through a 20 % sucrose cushion in TN buffer. The pellet was suspended in sterile TN buffer before being subjected to a subsequent cycle of concentration by passing through a 20 % sucrose cushion at 30000 RPM for 2 h at 4 °C. The pellet was suspended in 0.25 ml of sterile, endotoxin-free TN buffer and promptly chilled for use in subsequent experiments. This approach provides a three-step 6-h purification process for NiV-VLPs, which are pleomorphic viruses. (B) Expression of HiBiT-tagged NiV-M protein in purified NiV-VLP-1, NiV-VLP-2, as analyzed by N-Luc assay, 20 µg of LgBiT and its substrate was supplied exogenously. (C) Western blot analysis of 20 µg of denatured NiV-VLP1 and NiV-VLP2 respectively, showing the expression of NiV G and F (upper and middle panel); Expression of HiBiT tagged M protein was analyzed by HiBiT blotting (lower panel). Detection of NiV proteins G, F and M within NiV-VLPs by co-immunoprecipitation: (D) Purified NiV-VLP-1 or NiV-VLP-2 were immunoprecipitated with NiV G specific antibody and blotted for NiV F protein (E) Purified NiV-VLP-2 immunoprecipitated with NiV G/F specific antibodies and the expression of M protein was detected by HiBiT blotting using 20 µg LgBiT and substrate. Normal mouse IgG was used as control and 10 % of non-immunoprecipitated lysate served as inputs. (F) TEM analysis of purified NiV-VLPs documented with a JEOL-JEM 1010 microscope (100K magnification). (G) Titre of NiV-VLP2 generated in different batches normalized to Relative Light Units (RLU) by N-Luc assay. NiV-VLP1 served as secondary control (Error bars, mean ± SD, *P ≤ 0.05, **P ≤ 0.005, ***P ≤ 0.001, and ****P ≤ 0.0001, unpaired *t*-test). Uncropped/non-adjusted versions of western images are provided in supplementary information S3. Red boxes denote cropped images that are presented in the manuscript. (For interpretation of the references to colour in this figure legend, the reader is referred to the Web version of this article.)

3. Results

3.1. NiV structural proteins co-express and self-assemble to generate VLPs *in vitro*

VLPs offer a safer platform for handling and studying BSL-4 pathogens such as NiV *in vitro*. The codon optimized NiV-G, F, and M genes were commercially synthesized and cloned into the mammalian expression vector pcDNA3.1+ under the control of an enhanced CMV promoter. To produce HiBiT tagged NiV-VLPs, the reading frame encoding M protein was modified by appending a small 11 amino acid long peptide, HiBiT-either at the C- or N-terminus of the reading frame (referred to as M - C and M - N respectively) (Detailed in [Supplementary information S1 A](#)). The HiBiT, is a component of Nano-Luciferase (N-Luc) based split luciferase system which generates quantitative luminescence, upon complementation by an 18 kDa large fragment LgBiT [8]. As we haven't altered any amino acids in G, F, or proteins that are necessary for cell penetration, the protein post-translational modifications and functions will be identical to those of native Nipah virus proteins. Initially, all the expression vectors were validated by sequencing, and the integrity was further assessed using restriction digestion with specific set of restriction enzymes ([Supplementary information S1](#)).

To evaluate the expression of the viral proteins in cultured mammalian cells, exponentially growing HEK293T cells were individually transfected with plasmid constructs coding for distinct structural NiV proteins F, G, or M-C/M-N. Transfection using empty pcDNA3.1+ vector served as the control and the expressions of F and G proteins were determined respectively by Western blot analysis using antibodies specific to NiV F1 and G proteins ([Fig. 1A and B](#)) 48h post transfection. The expression of F and G proteins were further confirmed by immunofluorescence analysis using primary antibodies specific to NiV F and G proteins followed by secondary antibody conjugated to Alexa 594 ([Fig. 1C](#)). HiBiT-tagged M protein in cell lysate was detected by HiBiT blotting using the Nano-Glo assay system (Promega) with exogenous supply of 20 µg of LgBiT protein in the blotting buffer ([Fig. 1D](#)). The expression of M protein was also validated by luminometric microplate assay using LgBiT complementation as per manufacturer's instructions ([Fig. 1E](#)). Transfection and protein expression were validated in other cell lines as well.

NiV G and F proteins collectively retain assembly and budding capacity although it is much less efficient than that of the M protein containing VLPs [5]. Forging optimal-conditions for protein self-assembly and NiV-VLP formation, next we co-expressed the NiV structural proteins in combinations of G + F or G + F + M-C/M-N in HEK293T cells. The cell lysate and supernatant (SUP) were collected 48 h post-transfection. The co-expression of NiV proteins F, G, and M were validated in cell lysate respectively by Western blot analysis ([Fig. 1F and G](#)), HiBiT blotting ([Fig. 1H](#)) and N-Luc assays ([Fig. 1I](#)).

Thus, having confirmed that the NiV F, G, and M plasmids are co-expressed *in vitro*, we proceeded to large-scale transfections and NiV-VLP purification. The structural proteins assemble themselves *in situ* and the VLPs are released into the cell SUP. The co-expression, assembly and release of HiBiT tagged VLPs, as well as the of functioning HiBiT-LgBiT complementation system, are described in detail in [Fig. 1J](#). Transfections are done in combinations of G + F or G + F + M. The G + F VLP, which lacks the M protein, and the G + F + HiBiT M VLP, which expresses all three structural proteins, are respectively referred to as NiV-VLP-1 and NiV-VLP-2 hereafter in this manuscript. As an early attempt to evaluate the extracellular release of the nascent VLPs, instead of purifying, the collected cell-SUP was concentrated using Amicon MWCO filters (Merck) and utilized to infect HEK293T cells expressing LgBiT protein ([Fig. 1](#)).

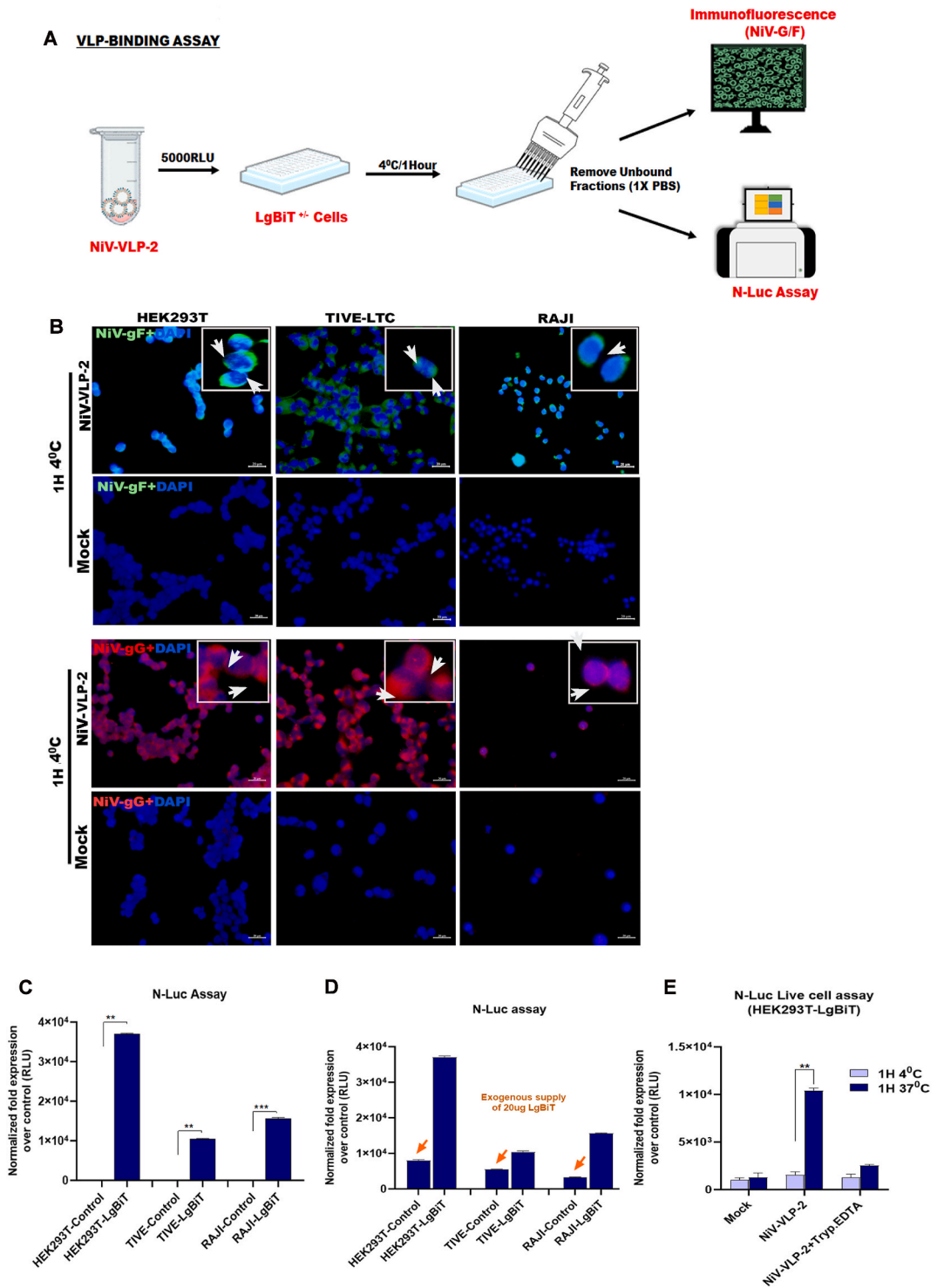
The luminescence resulting from the entry of suspected NiV-VLP-2 from the concentrated SUP was then detected by N-Luc assay. In comparison to the mock, cells infected with SUP from G + F + M-C/M-N transfected cells expressed higher luminosity ([Fig. 1K](#)), giving an initial trace of evidence on the extracellular secretion of nascent HiBiT tagged NiV-VLP2. Furthermore, the expression of HiBiT-M protein from SUP of cells transfected solely with the M expression plasmid was significantly lower than that of cells co-transfected with F, G, and M plasmids ([Fig. 1L](#)). These findings provided the first evidence on HiBiT tagged-NiV-VLP-2 genesis and its release in culture supernatants. Owing to the fact that both M-expression vectors (M - C and M-N, [Supplementary information S1A](#)) demonstrated equivalent properties, data from M-C will be shown in the further experiments (Represented as M).

3.2. Synthesis and purification of NiV-VLPs via a simple expedient approach

For a rapid production of substantial quantities of NiV VLPs *in vitro*, a less cumbersome three step approach was employed. The cell SUP collected 48h post co-transfection was exposed to sequential steps of clarification, purification and refining via ultracentrifugation through a 20 % sucrose cushion (Detailed in [Fig. 2A](#)). The cell SUP harvested from HEK293T cells transfected with empty vector pcDNA3.1+ and processed in similar way are referred to as mock. N-Luc assay was used to identify secreted NiV-VLP-1/2 ([Fig. 2B](#)). Western blot analysis for F and G proteins ([Fig. 2C](#), upper and middle panel), HiBiT blot for M protein ([Fig. 2C](#), lower panel) revealed that the NiV-VLP-1 expressed G and F proteins, whereas the HiBiT tagged NiV-VLP-2 was composed of G, F, and M proteins. Immunoprecipitation with F and G proteins and HiBiT blot for M protein further verified the expression and protein interactions of F, G and M proteins within the NiV-VLPs ([Fig. 2D and E](#)).

The morphogenic similarity of the VLPs to native NiV was then confirmed by transmission electron microscopy, numerous virus-like particles of varied sizes were spotted ([Fig. 2F](#)). The size variations of these VLPs were consistent with the native virus; NiV is a pleomorphic virus with a size range of 40–1900 nm [11,12]. The particle size discrepancies could be explained to the random clustering of F, G or M proteins in altering concentrations at the plasma membrane, resulting in VLPs of varied sizes; i.e., the amount of F and G proteins within the VLPs can be modified by manipulating F and G expression levels in the host cell [19] ([Fig. 2](#)).

Thus, under optimized settings, we were able to generate significant quantities of NiV-VLP-1/VLP-2. Owing to the pleomorphic nature of NiV and NiV-VLPs, the conventional practice of concentrating precleared SUP using MWCO filters, size exclusion chromatography and subsequent density gradient centrifugation [5,13–16] had been eliminated and modified in the present study to minimize VLP-loss.



(caption on next page)

Since the transfections were transient in nature, the titre of NiV-VLP-2s harvested from different batches were not identical; thus, on the basis of their N-Luc activity following LgBIT complementation, VLP inputs from different batches were normalized to Relative Light Units (RLU) for use in downstream experiments (Fig. 2G). As the G-F containing VLP-1 (without HiBiT tag) did not elicit any luminescence (Fig. 2G), this was employed as a secondary or negative control as well as to assess background noises in all luminometric assays.

Fig. 3. HiBiT tagged NiV-VLPs elicits host cell binding, *in vitro*

(A) Schematic representation of host cell binding assay: Briefly, cells stably expressing and not expressing LgBiT protein were infected with 5000 RLU of NiV-VLP2 at 4 °C for 1 h to facilitate the VLP binding, unbound fractions were washed off and the cells were either fixed for immunofluorescence analysis of NiV-G/F proteins or lysed in Nano-Glo lysis buffer for N-Luc assay. (B) Immunofluorescence analysis of NiV-G and F protein expression of cell surface bound VLPs respectively in HEK293T, TIVE-LTC and RAJI cells. Mock infected and cells not expressing LgBiT served as respective controls. Arrows in boxed areas indicate NiV-VLP2 bound to the cell membrane (40X, scalebar 20 μm). (C) HEK293T, TIVE-LTC and RAJI cells stably expressing LgBiT were incubated with NiV-VLP2 at 4 °C. One hour post VLP binding, the cells were lysed and the luminescence intensity was measured using N-Luc assay. (D) The VLP binding and luminescence intensities in LgBiT non-expressing HEK293T, TIVE-LTC cell lysates were measured by exogenous supply of 20 μg LgBiT protein. (as indicated by blue arrows). (E) N-Luc *in situ* live cell assay in HEK293T-LgBiT cells following VLP-2 addition. Cells were kept at 4 °C for 1 h post infection to promote binding, and thereafter shifted to 37 °C. Cells treated with 0.25 % Trypsin EDTA to remove cell bound VLP fractions, served as a negative control. Uncropped/non-adjusted versions of western images are provided in supplementary information S3. Red boxes denote cropped images that are presented in the manuscript. (For interpretation of the references to colour in this figure legend, the reader is referred to the Web version of this article.)

3.3. HiBiT tagged NiV-VLPs elicit host cell binding and entry, *in vitro*

VLPs have long been recognized as effective quantitative platforms for studying viral binding and entry kinetics. However, the advent of NanoBiT technology and HiBiT tagged VLP is far more sophisticated. To investigate the host cell binding efficacy of HiBiT-VLP-2, HEK293T, TIVE-LTC and RAJI cells stably expressing and not expressing LgBiT protein were incubated with 5000 RLU of NiV-VLP-2 for an hour at 4 °C, to allow their attachment to the cells (See supplementary information S2 A-C for generation of stable cell lines expressing LgBiT). Following incubation, the binding was confirmed by both immunofluorescence and N-Luc assay (Fig. 3A). For immunofluorescence analysis the cells were washed, fixed and immuno-stained for NiV G and F proteins; the VLP binding was detected on the cell surface (Fig. 3B).

After cell lysis, the quantitative measure of the cell surface bound VLP fraction was scored further using the N-Luc assay. Owing to the HiBiT:LgBiT complementation on cell lysis, the cells stably expressing LgBiT produced significantly higher luminescence compared to control cells lacking LgBiT (Fig. 3C). However, exogenous administration of 20 μg of LgBiT protein to these LgBiT-deficient control cell lysates, resulted in luminescence signals. (Fig. 3D); thus confirming the VLP binding on cell surface. This N-Luc based approach was found to be a very sensitive and quantitative way of measuring NiV-VLP-2 binding, with the signals ranging up to 50-80-fold greater than the mock or background.

We conducted further experiments in HEK293T cells to establish that there is just surface binding and, no VLP entry and allied HiBiT activation at 4 °C. For this a live cell assay was performed in presence of live cell substrate vivazine as detailed elsewhere. To aid in VLP binding rather than entry, post-infection cells were maintained at 4 °C for 1 h and further shifted to 37 °C. The luminescence intensities were measured before and after temperature shift. During the 1-h incubation at 4 °C no VLP entry or luminescence was detected as anticipated. However, shifting the cells from 4 °C to 37 °C post infection significantly increased the viral entry and the resultant luminescence signals. Though, those cells treated with 0.25 % Trypsin EDTA to remove surface bound fractions of VLP, exhibited no indication of viral entry in comparison to the mock, even after the temperature shift; demonstrating that there is no VLP entry or HiBiT activation at 4 °C (Fig. 3E).

Binding on the cell's surface is not necessarily indicative of viral invasion or entry. The non-lytic Nano-Glo live cell assay was used to quantitatively assess the capacity of VLPs to enter the cells. To measure the kinetics of NiV-VLP-2 entry, LgBiT-expressing HEK293T, TIVE-LTC and RAJI cells were incubated with 5000 RLU NiV-VLP-2 at 37 °C for different time points in presence of a live cell substrate vivazine. The entry kinetics of VLPs were then measured by N-Luc live cell assay.

Analyzing the kinetics of NiV-VLP-2 by N-Luc assay revealed that entry of the virus peaked between 30 min and 2 h and progressively dropped until 4 h post infection in both HEK293T and TIV-LTC cells (Fig. 4A and B). However, the lymphocytic cell line RAJI was found to be non-susceptible to NiV-VLP-2 entry as reported elsewhere [20] (Fig. 4C). To further validate the VLP entry, LgBiT-expressing HEK293T and TIVE-LTC cells were mechanically lysed by physical disruption methods. Cells which were not lysed served as the control. The cells were then mixed with NiV-VLP-2 *in vitro*; and resultant luminescence was measured using N-Luc assay in presence of the substrate. Physically disrupted cells elicited higher luminescence in comparison to the un-disrupted control cells (Supplementary information S2 D, E); i.e., cell lysis or VLP entry are the only ways to achieve HiBiT:LgBiT complementation and allied luminescence. This proved that HiBiT:LgBiT complementation occurs exclusively during NiV-VLP-2 entry in live cells, and the observed luminescence was neither induced by any unbound fractions of NiV-VLP-2 or HiBiT, nor was it caused by the presence of damaged cells. Comparing the results from lytic and live cell assays, on an average 20–60 % VLPs effectively entered target cells between 30mins and 2 h of incubation period.

However, to prove that the entry of VLPs is not altered by HiBiT tag, and it merely act as a tracking peptide, we performed additional experiments. For this immunofluorescence analysis was performed in HEK293T cells. Exponentially growing cells were infected with equal units of either NiV-VLP-1 (G + F-VLP/without a HiBiT tag) or NiV-VLP-2 (G + F + HiBiT M) at 37 °C. Cells were fixed and stained for NiV G and F proteins following infection to assess the VLP entry. Cells infected with both the VLPs elicited identical fluorescence intensities and revealed the presence of NiV proteins in the cytoplasm as proof of VLP entry (Fig. 4D). This indicates that HiBiT is merely a tracking peptide and that the presence or absence of the HiBiT tag has no effect on the viral or VLP entry mechanism.

As a result, HiBiT-tagged VLPs serves as a a quick and sensitive platform to concurrently investigate viral binding and entry into target cells.

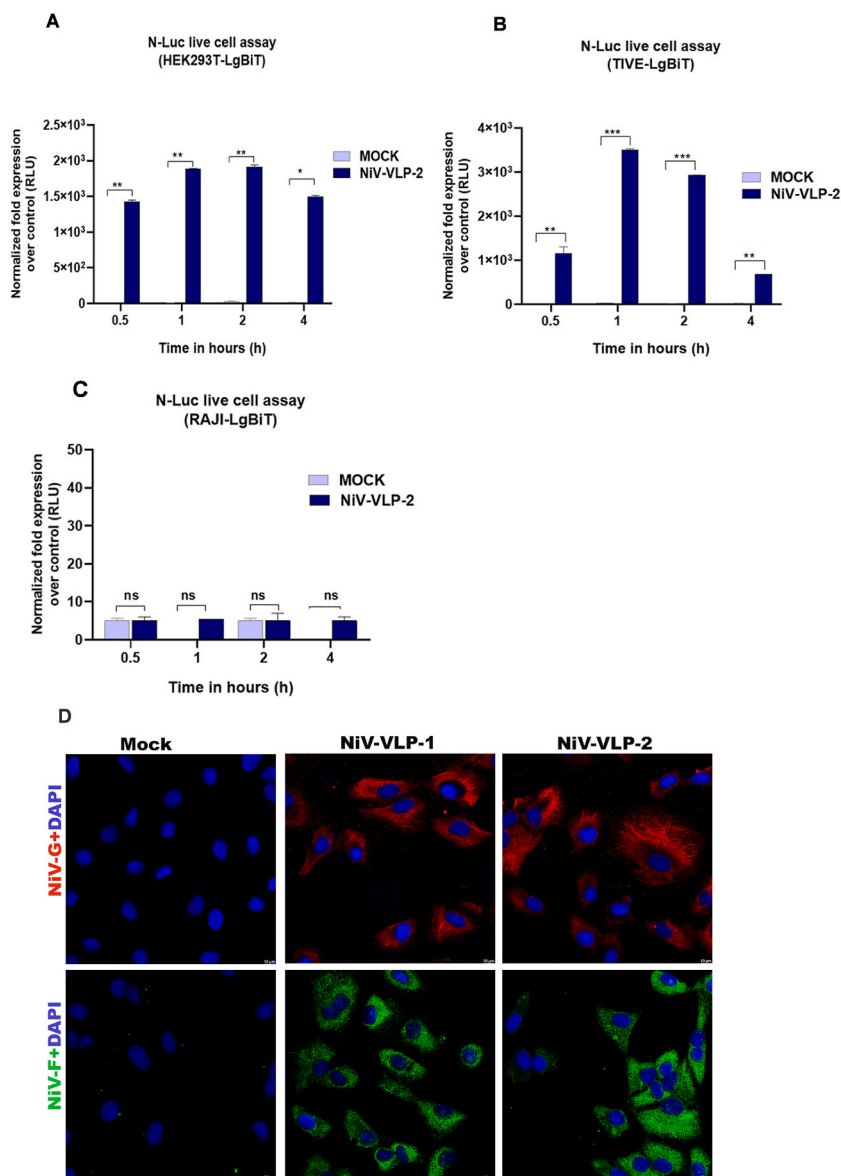


Fig. 4. HiBiT tagged NiV-VLPs elicit host cell entry, *in vitro* NiV-VLP2 host cell entry kinetics as measured by N-Luc in situ live cell assay in HEK293T (A), TIVE-LTC (B) and RAJI (C) cells stably expressing NanoLuc-LgBiT protein; in presence of live cell substrate Vivazine. The luminescence intensity was measured at different time points and the intensities normalized to respective controls, are expressed in RLU. Mock infected cells as well as cells not expressing LgBiT served as respective controls for the assay. (D) Immunofluorescence analysis of NiV-G and F protein expression in HEK293T cells post infection with VLP-1 (G + F) and VLP-2 (G + F + HiBiT M) (Scale bar 10 μ m, 63X). (Error bars, mean \pm SD, * $P \leq 0.05$, ** $P \leq 0.005$, *** $P \leq 0.001$, **** $P \leq 0.0001$, unpaired *t*-test).

3.4. HiBiT tagged VLPs offer a platform for rapid antibody neutralization studies

From the above results, it is evident that NiV-VLPs possess all of the morphogenic and functional properties of the natural virus, making them a good candidate for vaccine or antiviral research. Screening of inhibitors or antibodies that can impede the viral entry, is the most promising approach in vaccine virology or antiviral therapies. NiV glycoprotein G interacts with cellular receptors, allowing viral entry into host cells. Antibodies against the NiV-G proteins are thus identified to be vital for clearing viral infection and vaccine-induced protective immunity [21]. Thus, we performed neutralization experiments to see if neutralizing antibodies might block the binding or entry of the HiBiT tagged NiV-VLP-2s. For this, the VLPs were preincubated at 37 $^{\circ}$ C with increasing doses of neutralizing or non-neutralizing monoclonal antibodies specific to NiV G protein. The VLP entry kinetics was then recorded in LgBiT expressing HEK293T, TIVE-LTC and RAJI cells, using N-Luc based live cell substrate vivazine.

As the internalization of VLPs assessed by luminometric assay, neutralizing antibody prevented the VLP entry into the host cell in a dose dependent manner with 65 %, 60 % and 76 % decrease in entry at 2, 5 and 10 μg concentrations of antibody, respectively, 2 h post infection. However, the non-neutralizing antibody did not significantly affect the VLP entry (Fig. 5A and B). To maximize the HiBiT: LgBiT complementation, after 2 h post infection, cells were lysed with Nano Glo lysis solution. The fraction of VLPs that entered cells over a 2h period was then calculated in relation to the luminescence acquired from lytic assay (Fig. 5C and D). Thus, on antibody-dependent neutralization, there was a considerable reduction in the proportion of VLPs entering the target cells, indicating that VLPs provide a potent platform for rapid antibody neutralization studies or other *in vitro* viral assays. The HiBiT tag on the VLPs made it simple and swift to differentiate between the VLP assembly, release, host cell binding and entry without the need of antibodies or other complex assays.

4. Discussion

The BSL-4 pathogen NiV, causes incredibly fatal and potentially debilitating disease in humans. Thus, the protection of humans through restorative or prophylactic therapy or effective vaccination is a public health priority. Since viral entry is the most important step in the process of infection, screening of antibodies or antivirals that could possibly prevent entry will help us to develop the most

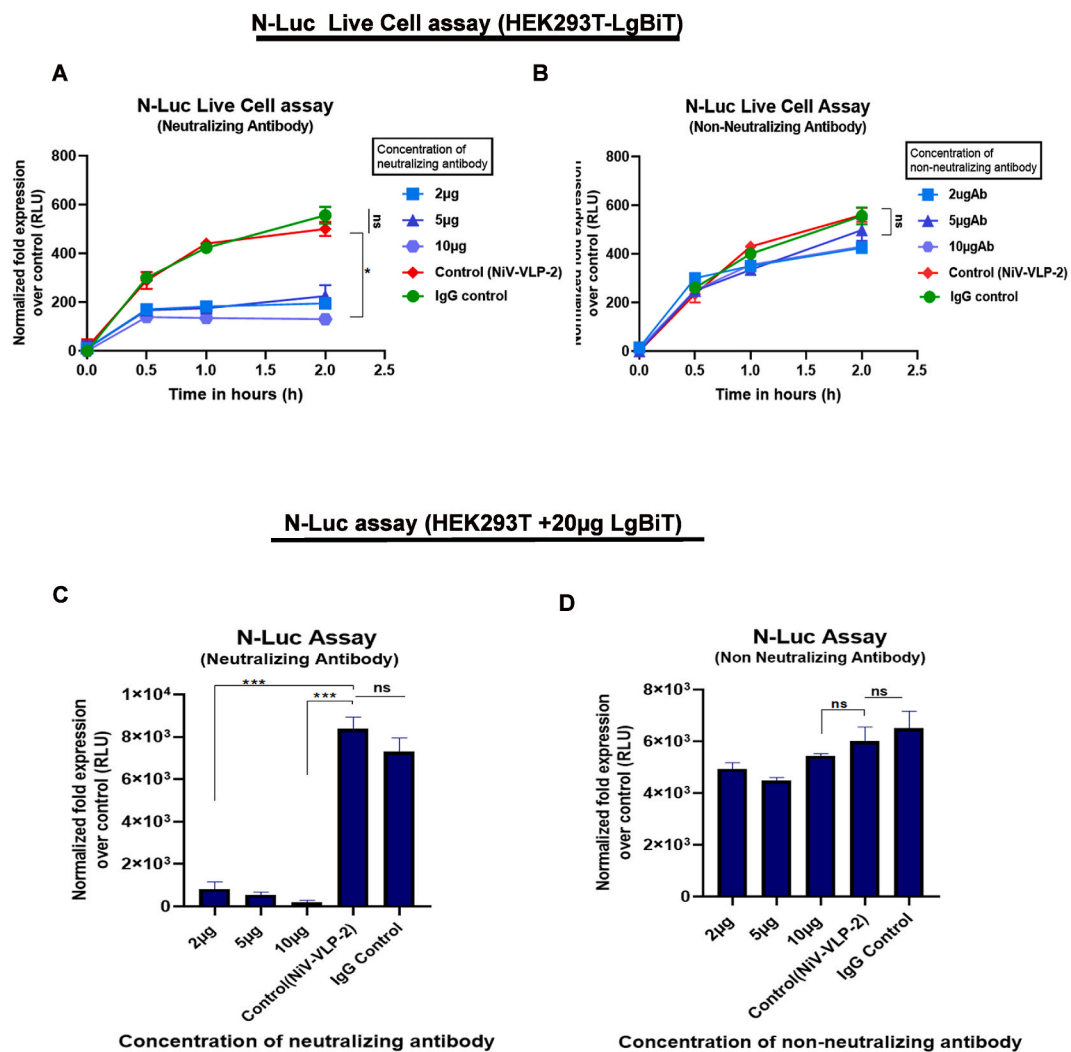


Fig. 5. HiBiT tagged VLPs offers a platform for rapid antibody neutralization studies 5000 RLU of NiV-VLP2 were left untreated (NiV-VLP-2 alone) or treated with 2, 5 and 10 μg of NiV-G neutralizing (A) or non-neutralizing antibodies (B) at 37 °C. Following neutralization, the LgBiT-expressing HEK293T cells were infected with untreated as well as antibody treated NiV-VLP-2, and the viral entry kinetics was examined at various time points using the N-Luc *in situ* live cell assay, as previously described. NiV-VLP-2 treated with equivalent concentrations of normal mouse IgG served as the control. Parallely, cells were lysed post treatment and the fraction of VLPs that entered cells over a 2h period was then calculated by lytic assay (C, D). Error bars, mean \pm SD, * $P \leq 0.05$, ** $P \leq 0.005$, *** $P \leq 0.001$, and **** $P \leq 0.0001$, unpaired *t*-test).

effective strategies for the treatment of NiV infection. However, the pathogenicity and the need for biocontainment laboratories limits the research on NiV. Here we introduce a safe and economic way of producing HiBiT-tagged NiV -VLPs mimicking the wild type virus, using a less cumbersome approach. By incorporating the NanoBiT technology into the NiV-VLP platform, we were able to concurrently dissect both host cell binding as well as the entry kinetics of NiV. Moreover, they also offered a platform for rapid antibody neutralizations.

To assist *in situ* assembly and release of nascent NiV VLPs, NiV G, F, and M expressing plasmids were co-transfected into exponentially growing HEK293T cells. The addition of the HiBiT tag to the ORF for M protein elicited the production of HiBiT tagged VLPs and made their detection, quantification, and downstream studies easier with LgBiT complementation as mentioned elsewhere [8,9]. In recognition of the possibility that, over expression of the matrix M protein could lead to higher order self-assembly and its autonomous release even in the absence of F and G, equimolar concentrations of plasmids were utilized for transfection. Furthermore, reduced M protein expression has been shown to influence stability, structure, incorporation of F, G and infectivity of VLPs [19,22]. Thus, equimolar quantities of plasmid were employed to minimize the atypical or unconventional release of nonspecific VLPs. Transfections were done in combinations of G + F or G + F + M. Concurrently, we could also detect higher order clusters of M protein in HiBiT blot experiments (Fig. S2 F).

The reported transfection efficiencies of HEK293T cells ranges between 85 and 99 %. Owing to this high transfection efficiency, high protein production and lower doubling time all our transfection-based assays for large scale production of VLPs employed HEK293T cells. Harvesting and purifying VLPs from transfected cell SUP was accomplished in three simple steps. Owing to the pleomorphic nature of NiV and NiV-VLPs, the conventional practice of concentrating precleared SUP using MWCO filters, size exclusion chromatography and subsequent density gradient centrifugation [5,13–16] had been eliminated and modified in the present study to minimize VLP-loss. And thus, we were able to generate considerable quantities of NiV VLPs (NiV-VLP-1 and HiBiT tagged NiV-VLP-2) apparently mimicking their native virus, as detected by luminometric assays and TEM analysis.

Numerous particles of varied sizes were spotted in TEM analysis; NiV is a pleomorphic virus with a size range of 40–1900 nm [11, 12] and thus the size variations of these VLPs were consistent with the native virus. The particle size discrepancies can also be attributed to the random clustering of F, G or M proteins in altering concentrations at the plasma membrane, resulting in VLPs of varied sizes; i.e., The quantity of F and G proteins adhering to M protein clusters can be manipulated by altering F and G expression levels in cells leading to the production of chemically and morphologically distinct VLPs [19].

The titer and total protein concentration, of VLPs from different batches varied and was normalized to Relative Light Units (RLU) based on their N-Luc activity or luminescence intensity after LgBiT complementation, which enabled the elimination of omissions in subsequent experiments.

As it was confirmed that HiBiT-M VLPs (NiV-VLP-2) structurally mimicking native virus were formed, their cell binding ability was assessed further. The purified VLPs were allowed to bind on to HEK293T, TIVE-LTC and RAJI cells at 4 °C. Immunofluorescence labelling with NiV G and F antibodies revealed the presence of VLP on the cell surface. The lysis of target cells along with the bound VLP fraction, followed by LgBiT complementation, permitted maximum luminescence as determined by the N-Luc assay.

Epithelial and endothelial cells in blood vessels are the primary biological targets for NiV and thus endothelial cell line TIVE-LTC and epithelial cell line HEK293T were chosen [23]; RAJI cells, on the other hand, are reported to be NiV-non-susceptible and were employed as control cells [20]. However, VLP binding was seen in all of the cell lines, confirming their virus-like characteristics.

The VLP systems presented here also serve as platforms to evaluate virus-cell entry. We spotted that the HiBiT tags used to track VLP genesis and host cell binding may also be employed to measure VLP-cell entry kinetics; and the N-Luc based live cell assay was utilized for this. Comparing the results from lytic and live cell assays, on an average 20–60 % of VLPs effectively entered target cells between 30mins and 2 h of incubation period. Yet, as anticipated VLP entry was not observed in RAJI cells, supporting the notion that cell surface binding is not necessarily indicative of viral invasion or entry. Thus, it is logical to speculate that the lymphocytic cells might serve as vehicles for NiV, that the virus 'hitch and ride', these cells initiating an infection in the endothelial cells and disseminating to different parts of the body including central nervous system [24]. This has been proved *in vitro* by Tiong et al., by demonstrating the *trans*-endothelial migration of infectious immature dendritic cells [25]. This sensitive NanoBiT technology-based system can thus be concurrently used to dissect both the virus binding and virus-cell entry. The low RLU rates or inconsistencies in RLU observed across trials, however, could be attributed to the fact that only 5000 RLU of VLP inputs were used for each test, which is a significantly low quantity and might skew the cumulative luminescence.

We performed neutralization experiments to see if neutralizing antibodies might block the binding or entry of the HiBiT tagged VLPs, by preincubating the VLPs with different concentrations of NiV G specific neutralizing and non-neutralizing monoclonal antibodies. Thus, on antibody-dependent neutralization, there was a considerable reduction in the proportion of VLPs entering the target cells, indicating that VLPs provide a potent platform for rapid antibody neutralization assays. As a result, the form and nature of the generated VLPs appeared to be comparable to those of the native virus. Extensive and rigorous studies are needed to emphatically show the efficacy of these VLPs, although this report is the initial of its kind using HiBiT tagged NiV-VLPs demonstrating their application in neutralization assays.

Overall, we report a simple system for generating HiBiT-VLPs which can be utilized in a BSL-2 laboratory, to concurrently quantify features of NiV assembly, binding and entry. This also offers an alternate-safe and effective platform for viral based antibody neutralization assays *in vitro*. The potential risks of using native viruses in viral host interaction assays, immune response studies, immunoglobulin validations and other viral-based assays could be alleviated with the use of these HiBiT tagged VLPs. Thus, the antigenicity and allied vaccine potential of these particles would serve as the base for future investigations involving *in vivo* models for not just NiV but also other potentially pathogenic viruses.

A number of paramyxoviruses, including those that cause human parainfluenza virus 3/5, measles virus, Newcastle disease virus,

Sendai virus, Nipah virus, and Hendra virus, have been extensively utilized in vaccine virology, *in vitro* assays, and even as targeted cargoes owing to their ability to form VLPs. However, Hendra and Nipah viruses are the most virulent BSL-4 pathogens among these paramyxoviruses; and neither preventative nor therapeutic measures exist for human infections. Therefore, although the concept of generating VLPs or tagged VLPs (e.g., HiBiT) is applicable to all of these viruses, it is particularly advantageous to apply this strategy to BSL-3/4 viruses, which are relatively unstudied owing to their elevated pathogenicity, as they can be handled in a BSL-2 facility. Nevertheless, the notion of tagged VLPs is not limited to paramyxoviruses; it also encompasses other enveloped viruses [26].

5. Conclusion

Nipah virus (NiV) research is currently restricted to BSL-4 laboratories. As a result, the fundamental mechanism of viral entry and allied pathogenicity has received little attention. Thus, understanding the precise process of viral particle formation and host cell entry is crucial in developing targeted therapy or particle-based vaccines. The BSL-2, replication-incompetent system offered by NiV-VLPs can be utilized to assess virus assembly, as well as the mechanisms of virus-cell interaction and entry, in cultured cells *in vitro*. We report a NiV-VLP system that exploits nanoluciferase (N-Luc) fragment complementation for tracking the assembly and *in vitro* entry, utilizing a NanoBiT technology. A simple three-step technique generated significantly large quantities of HiBiT-NiV VLPs that could be handled in a BSL-2 laboratory. The VLPs produced were morphologically and functionally identical to the parent virus, and the HiBiT-tag allowed for its rapid application in viral binding, cellular entry and antibody neutralization tests, further accelerating their potential in antiviral drug screening and vaccine development. The NiV-VLP platforms have a great deal of potential for further development towards prophylactic usage in humans, as evidenced by the fact that the VLPs also include viral surface proteins in their native state, which enables the VLPs to induce the formation of properly reactive antibodies. While many other paramyxoviruses have been extensively studied for their ability to assemble and generate VLP, the use of tagged VLP platforms for neutralization or other *in vitro* viral assays is still an area that has yet to be explored. Thus, we strongly advocate that this approach be used in studies on potent BSL-3/4 paramyxoviruses other than Nipah virus.

Limitation of the study

While we were successful in producing significant amounts of HiBiT tagged NiV VLPs, the transfections were transient in nature, limiting the yields and variability in titre of each batch of VLP, so selecting a population of cells stably expressing all three structural proteins would have been advantageous and time saving. Furthermore, employing negatively stained VLP preparations for TEM examination would have provided precise structural details of the VLPs. Although this is a novel and constructive report using HiBiT tagged NiV-VLPs demonstrating their application in neutralization assays, extensive and rigorous studies using multiple neutralizing antibodies and antivirals that block entry of the virus are needed to conclusively show the efficacy of these VLPs.

Data availability statement

Data generated out of this study is included in article/supplementary material/referenced in article.

CRediT authorship contribution statement

Arathi Rajan: Writing – original draft, Visualization, Methodology, Investigation, Formal analysis. **Anuja S. Nair:** Methodology, Investigation. **Vinod Soman Pillai:** Methodology, Investigation. **Binod Kumar:** Methodology. **Anupama R. Pai:** Methodology, Investigation. **Bimitha Benny:** Methodology, Investigation. **Mohanan Valiya Veetil:** Writing – review & editing, Supervision, Project administration, Investigation, Funding acquisition, Formal analysis, Conceptualization.

Declaration of competing interest

The authors declare that they have no known competing financial interests or personal relationships that could have appeared to influence the work reported in this paper.

Acknowledgements

We thank Dr. Rolf Renne (University of Florida) for providing endothelial cell line TIVE-LTC. This work was supported by Institute of Advanced Virology internal research fund. ANS thanks the Department of Biotechnology, Government of India for fellowship.

Appendix A. Supplementary data

Supplementary data to this article can be found online at <https://doi.org/10.1016/j.heliyon.2024.e31905>.

References

- [1] S. Banerjee, et al., Nipah virus disease: a rare and intractable disease, *Intractable Rare Dis Res* 8 (1) (2019) 1–8.
- [2] V. Soman Pillai, G. Krishna, M. Valiya Veettil, Nipah virus: past outbreaks and future Containment, *Viruses* 12 (4) (2020).
- [3] S. Banerjee, et al., First experience of ribavirin postexposure prophylaxis for Nipah virus, tried during the 2018 outbreak in Kerala, India, *J. Infect.* 78 (6) (2019) 491–503.
- [4] R. Chandni, et al., Clinical manifestations of Nipah virus-infected patients who presented to the emergency department during an outbreak in Kerala state in India, may 2018, *Clin. Infect. Dis.* 71 (1) (2020) 152–157.
- [5] P. Walpita, et al., Vaccine potential of Nipah virus-like particles, *PLoS One* 6 (4) (2011) e18437.
- [6] B.H. Harcourt, et al., Genetic characterization of Nipah virus, Bangladesh, 2004, *Emerg. Infect. Dis.* 11 (10) (2005) 1594–1597.
- [7] B.H. Harcourt, et al., Molecular characterization of Nipah virus, a newly emergent paramyxovirus, *Virology* 271 (2) (2000) 334–349.
- [8] M. Sasaki, et al., Development of a rapid and quantitative method for the analysis of viral entry and release using a NanoLuc luciferase complementation assay, *Virus Res.* 243 (2018) 69–74.
- [9] B. Kumar, et al., Assembly and entry of severe acute respiratory syndrome coronavirus 2 (SARS-CoV2): evaluation using virus-like particles, *Cells* 10 (4) (2021).
- [10] M.K. Schwinn, et al., CRISPR-mediated tagging of endogenous proteins with a luminescent peptide, *ACS Chem. Biol.* 13 (2) (2018) 467–474.
- [11] A.D. Hyatt, et al., Ultrastructure of Hendra virus and Nipah virus within cultured cells and host animals, *Microbes Infect* 3 (4) (2001) 297–306.
- [12] C.S. Goldsmith, et al., Elucidation of Nipah virus morphogenesis and replication using ultrastructural and molecular approaches, *Virus Res.* 92 (1) (2003) 89–98.
- [13] G.P. Johnston, et al., Nipah virus-like particle egress is modulated by cytoskeletal and vesicular trafficking pathways: a validated particle proteomics analysis, *mSystems* 4 (5) (2019).
- [14] H.D. Pantua, et al., Requirements for the assembly and release of Newcastle disease virus-like particles, *J. Virol.* 80 (22) (2006) 11062–11073.
- [15] P. Walpita, et al., A VLP-based vaccine provides complete protection against Nipah virus challenge following multiple-dose or single-dose vaccination schedules in a hamster model, *NPJ Vaccines* 2 (2017) 21.
- [16] E. Qing, et al., Inter-domain communication in SARS-CoV-2 spike proteins controls protease-triggered cell entry, *Cell Rep.* 39 (5) (2022) 110786.
- [17] A. Rajan, et al., Modulation of BRCA1 mediated DNA damage repair by deregulated ER-alpha signaling in breast cancers, *Am. J. Cancer Res.* 12 (1) (2022) 17–47.
- [18] X.Y. Liang, et al., Development of HiBiT-tagged recombinant infectious bronchitis coronavirus for efficient in vitro and in vivo viral quantification, *Front. Microbiol.* 11 (2020) 2100.
- [19] Q. Liu, et al., A stochastic assembly model for Nipah virus revealed by super-resolution microscopy, *Nat. Commun.* 9 (1) (2018) 3050.
- [20] O.A. Negrete, et al., EphrinB2 is the entry receptor for Nipah virus, an emergent deadly paramyxovirus, *Nature* 436 (7049) (2005) 401–405.
- [21] G. Kalodimou, et al., A soluble version of Nipah virus glycoprotein G delivered by vaccinia virus MVA activates specific CD8 and CD4 T cells in mice, *Viruses* 12 (1) (2019).
- [22] R.E. Watkinson, B. Lee, Nipah virus matrix protein: expert hacker of cellular machines, *FEBS Lett.* 590 (15) (2016) 2494–2511.
- [23] K.T. Wong, et al., Nipah virus infection: pathology and pathogenesis of an emerging paramyxoviral zoonosis, *Am. J. Pathol.* 161 (6) (2002) 2153–2167.
- [24] E.C.W. de Boer, J.M. van Gils, M.J. van Gils, Ephrin-Eph signaling usage by a variety of viruses, *Pharmacol. Res.* 159 (2020) 105038.
- [25] V. Tiong, et al., Nipah virus infection of immature dendritic cells increases its transendothelial migration across human brain microvascular endothelial cells, *Front. Microbiol.* 9 (2018) 2747.
- [26] S. Panthi, et al., Paramyxovirus-like particles as protein delivery vehicles, *J. Virol.* 95 (20) (2021) e0103021.